Transition Probabilities for Low-Lying States in ^{92}Nb†

S. Cochavi and D. B. Fossan
Department of Physics, State University of New York, Stony Brook, New York 11790
(Received 7 August 1970)

Low-lying states in ^{92}Nb have been studied using the ^{92}Zr$(p, n\gamma)^{92}$Nb reaction at $E_p = 6.3$ MeV. A Ge(Li) γ spectrum was measured in coincidence with neutrons to identify low-lying states and their γ transitions. The mean lifetime of the 357-keV state was measured as $\tau = 2.73 \pm 0.09$ nsec by a neutron-γ delayed-coincidence technique. The mean lifetime of the 227-keV 2^- state obtained from a γ-γ delayed-coincidence measurement is $\tau = 6.2 \pm 0.7$ μsec. An upper limit of $\tau \leq 0.8$ nsec was measured for the mean lifetime of the 501-keV state. These lifetime results and observed γ transitions established for the predicted $[\pi, \frac{9}{2}^+] [\nu(2d_{5/2})] J^+$ configuration the level sequence 7^+, 2^+, 3^+, 5^+, 4^+, 6^+. A $B(E2) = 50.9\ e^2\,\mathrm{F}^4$ was deduced for the $5^+ \rightarrow 7^+$ (357→0 keV) transition from the lifetime of the 357-keV state; effective $E2$ charges for the mass-90 region are compared. The lifetime of the 2^- state implies an $E1$ hindrance of 10^7 for the $2^- \rightarrow 2^+$ (227→135 keV) γ transition relative to single-particle estimates.

I. INTRODUCTION

The nucleus $^{92}_{41}\mathrm{Nb}_{51}$ has been the subject of a considerable number of theoretical and experimental studies[1-10] in recent years. According to jj-coupling shell-model theory, protons in the $38 < Z \leq 50$ region are either in the $2p_{1/2}$ or $1g_{9/2}$ orbits, and neutrons in the $50 < N \leq 56$ region are in the $2d_{5/2}$ orbit. For the ^{91}Nb nucleus with a closed shell of 50 neutrons, it suggests a ground-state proton configuration of $[\pi_0, \frac{9}{2}^+] = [a(2p_{1/2})^2(1g_{9/2}) + b(1g_{9/2})^3, \frac{9}{2}^+]$, and for the first excited state at 104 keV a proton configuration of $[\pi_1, \frac{1}{2}^-] = [(1g_{9/2})^2(2p_{1/2}), \frac{1}{2}^-]$. The addition of a $2d_{5/2}$ neutron to ^{91}Nb in this model should give rise to low-lying states in ^{92}Nb with configurations $[\pi_0, \frac{9}{2}^+][\nu(2d_{5/2})]J^+$, where $J = 2$, 3, 4, 5, 6, 7, and $[\pi_1, \frac{1}{2}^-][\nu(2d_{5/2})]J^-$, where $J = 2$, 3.

The six positive-parity states of the configuration $[\pi_0, \frac{9}{2}^+][\nu(2d_{5/2})]J^+$ have been observed in neutron pickup reactions by Sheline, Watson, and Hamburger[1] with ^{93}Nb(d, t) and by Sweet, Bhatt, and Ball[2] with ^{93}Nb(p, d). These states have also been studied recently by Cates, Ball, and Newman[3] via the ^{91}Zr$(^3\mathrm{He}, d)^{92}$Nb reaction and were found to exhibit predominantly $l = 4$ angular distributions. The energies of these states were determined to within 5 keV. Tentative spin assignments for the observed states have been based on a qualitative comparison of these experimental results with theoretical calculations of de-Shalit[4] and of Kim.[5] The level order so assigned is 7^+, 2^+, 5^+, 3^+, 4^+, and 6^+. The ordering of the 3^+ and 5^+ and that of the 4^+ and 6^+ levels are not well defined by the relative yields to these levels. The only ^{92}Nb state with a firmly established spin and parity is the 135-keV 2^+ state which decays, with a mean lifetime[11,12] of $\tau = 14.7$ days, by electron capture and positron emission to two 2^+ states in ^{92}Zr. The 7^+ assignment for the ^{92}Nb ground state is consistent with its lifetime and that of the 135-keV state in addition to the reaction information.

The 2^- and 3^- levels expected in ^{92}Nb from $[\pi_1, \frac{1}{2}^-][\nu(2d_{5/2})]J^-$ have been predicted by Auerbach and Talmi[6] to have energies of 0.2 and 0.4 MeV, respectively. This negative-parity doublet was not populated by the neutron-pickup reactions. Two low-lying $l = 1$ states were reported at 0.23 and 0.39 MeV by Cates, Ball, and Newman[3] using the ^{91}Zr$(^3\mathrm{He}, d)^{92}$Nb reaction. Assignments of 2^- to the 0.23-MeV state and 3^- to the 0.39-MeV state were based on the relative yields for this reaction.

The level order of the positive-parity sextuplet of levels in ^{92}Nb, as yet undefined, plays an important role in defining the effective interaction between a $1g_{9/2}$ proton and a $2d_{5/2}$ neutron and thus in the prediction of the level structure and properties of nuclei in the region $38 < Z < 50$, $50 < N < 56$. For example, the low-lying levels in isotopes of Nb, Mo, and Tc arising from the coupling of protons in the $1g_{9/2}$ orbit and neutrons in the $2d_{5/2}$ orbit have been calculated[6-8] by the use of an effective interaction defined by the experimental level spectra of ^{92}Zr, ^{92}Mo, and ^{92}Nb. For these calculations, Auerbach and Talmi[6] used the positive-parity levels in ^{92}Nb with the above level order except for the exchange of the 3^+ and 5^+ levels. The calculations by Vervier[8] and by Sheline *et al.*[9] were done assuming both of these level orders, and Vervier, in addition, made exchanges in the 4^+ and 6^+ levels. Pandya[10] has shown that the spin sequence 7^+, 2^+, 5^+, 3^+, 4^+, 6^+ cannot be reproduced by a central residual potential with a reasonable range; instead a level order of 7^+, 2^+, 3^+, 5^+, 4^+, 6^+ is preferred.

The purpose of the present experiment is to investigate electromagnetic transitions between low-lying states in ^{92}Nb in order to obtain further information on the nuclear structure and spin assign-

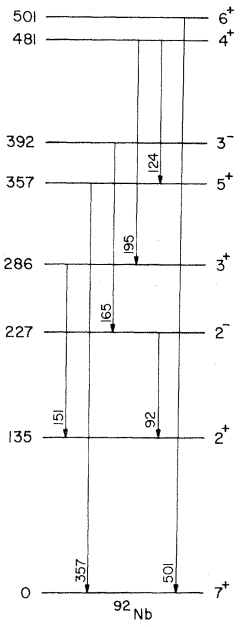

FIG. 1. Prominant γ-ray transitions observed in ^{92}Nb. The level scheme and spin-parity parameters are consistent with this work and that of Cates, Ball, and Newman. Energies are in keV.

ments for these states. The level order of the 3^+ and 5^+, and 4^+ and 6^+ states is especially important for the above mentioned theoretical predictions of low-lying states for nuclei with $38 < Z < 50$ and $50 < N < 56$. An interesting aspect of this study involves transitions between the positive-parity sextuplet of states and the negative-parity doublet. Because an $E1$ transition is forbidden between $2p_{1/2}$ and $1g_{9/2}$ configurations, a measurement of the $E1$ transition probabilities between these two groups of levels makes a sensitive test regarding the purity of the suggested configurations.

II. EXPERIMENTAL METHOD

A. ^{92}Zr$(p, n\gamma)^{92}$Nb; Singles and Neutron-Coincidence γ Spectra

The low-lying levels of ^{92}Nb are shown in Fig. 1. In order to determine which levels are significantly populated in the ^{92}Zr$(p, n\gamma)$ reaction, a preliminary investigation was made in singles with a Ge(Li) γ-ray detector. The γ rays produced by bombarding a ~1-mg/cm^2 self-supporting ^{92}Zr metal target with 6.30-MeV protons were measured with a 30-cc Ge(Li) detector placed at 90° to the beam direction. The detector energy resolution was approximately 3.8 keV for the 1.332-MeV ^{60}Co γ ray. Figure 2 shows the resulting γ-ray spectrum.

In order to isolate the electromagnetic transitions in ^{92}Nb, the γ spectrum in coincidence with neutrons was also measured. The neutron detec-

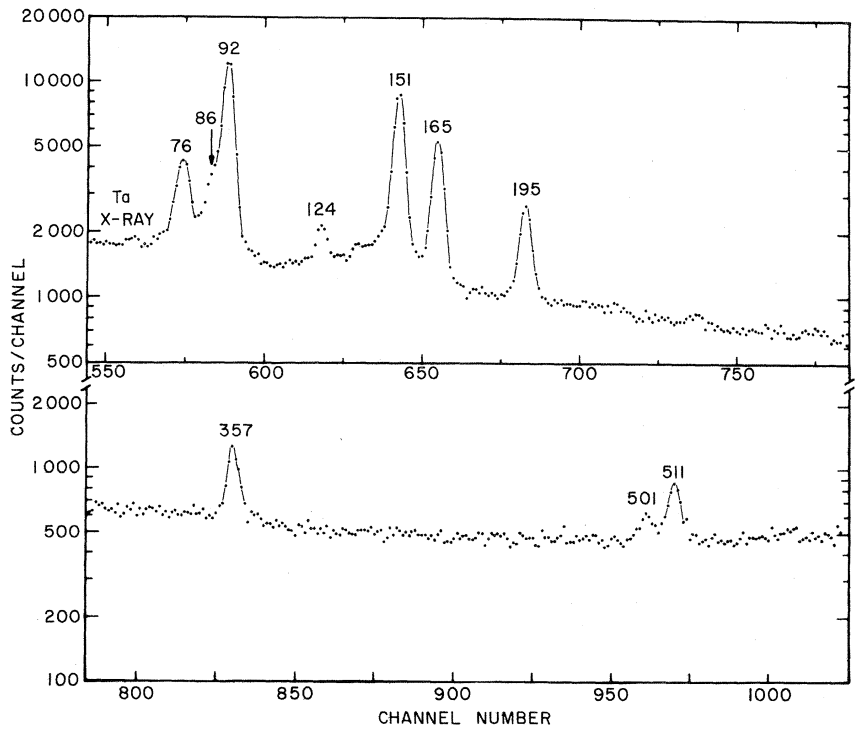

FIG. 2. γ-ray singles spectrum obtained for 6.3-MeV protons bombarding a thin self-supporting metal target of ^{92}Zr. The Ge(Li) detector was placed at 90° to the beam axis. The γ energies in keV units are written above the peaks.

tor was a 2×2-in. NE 213 liquid scintillator coupled to an RCA 8575 photomultiplier tube. Its axis was placed at 20° to the beam direction. A disk of lead, 0.12 in. thick, was placed in front of the neutron detector to attenuate low-energy γ rays. Neutron-γ pulse-shape discrimination was used to select the neutrons.[13]

The basis of the neutron-γ pulse-shape discriminator is the NE 213 scintillator. This scintillator material has two dominant decay times, a fast time $\tau < 4$ nsec and a slow decay time $\tau \sim 300$ nsec. Neutron-induced proton recoils produce a larger amount of the long-lived component than do γ-induced Compton electrons. The time difference between the initial fast component as observed at the anode and the bipolar crossover of the time-integrated linear pulse from a dynode is thus different for neutrons and γ rays. A measurement of this time difference for each pulse with a time-to-amplitude converter (TAC), allows the selection of only neutrons. The neutron-γ pulse-shape discriminator is shown in the right part of Fig. 3. A typical time-difference spectrum discussed above which shows the separation of the neutrons and γ rays is displayed in Fig. 4. The single-channel analyzer (SCA) 2 is adjusted to select from TAC 1 the pulse-height region appropriate to neutrons.

The Ge(Li) γ spectrum taken in coincidence with neutrons for the ^{92}Zr$(p, n\gamma)^{92}$Nb reaction is shown in the lower portions of Figs. 5 and 6. A singles γ-ray spectrum for ^{92}Zr$+p$ is shown for comparison purposes in the upper portions of the same figures with identical gain and dispersion. For this neutron-coincidence measurement, the random events were measured and subtracted from the spectrum. A large coincidence resolution time of ~200 nsec was intentionally used in order to include with some efficiency γ rays of long-lived states ($\tau \sim 0.5$ μsec). Figures 5 and 6 show that most of the prominent peaks in the singles spectrum with energy up to 540 keV are from the ^{92}Zr$(p, n\gamma)^{92}$Nb reaction. The γ rays associated with ^{92}Nb correspond to γ transitions as shown in Fig. 1. The error in the energies of the transitions is approximately ~1 keV. Figure 5 shows that the 392-keV 3^- state cascades via the 165-keV γ ray to the 227-keV 2^- state and the latter decays by the 92-keV γ ray to the 135-keV 2^+ state. These γ rays were used for the lifetime measurement of the 227-keV 2^- state. The relative yields of the 92-keV γ ray in the singles and the coincidence spectra indicate that the lifetime of the 227-keV 2^- state is greater than the coincidence resolving time. The 357- and 501-keV γ rays correspond, respectively, to the ground-state decay of the 357-keV (5^+) and the 501-keV (6^+) states; these γ rays were used for the lifetime measurements of the respective states.

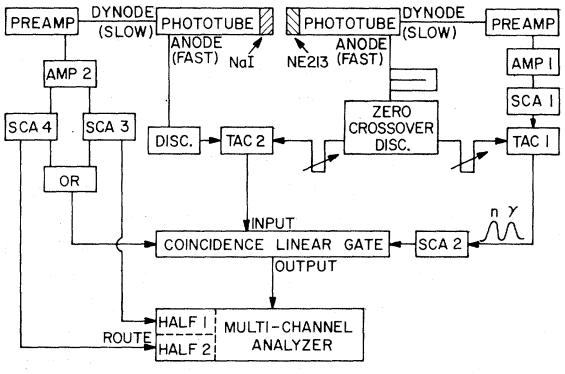

FIG. 3. A schematic diagram of the experimental apparatus.

B. Lifetime Measurement of the 357-keV (5^+) and 501-keV (6^+) States

The lifetime of the 357-keV (5^+) state was measured by a neutron-γ delayed-coincidence technique. An excitation study of the γ rays from the ^{92}Zr$(p, n\gamma)^{92}$Nb reaction was made with a Ge(Li) detector for proton energies between 5.0 and 8.5 MeV. The optimum energy chosen for the lifetime measurement of this state was ~6.3 MeV. At this proton energy, the neutrons corresponding to the excitation of the state have an energy of ~3.1 MeV at

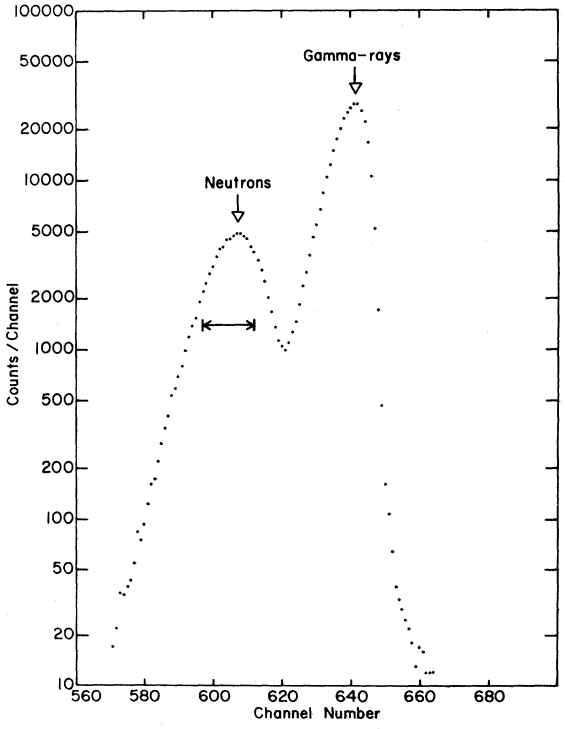

FIG. 4. Pulse-height spectrum from TAC 1 showing discrimination spectrum of neutron and γ-ray pulses with NE 213 liquid scintillator.

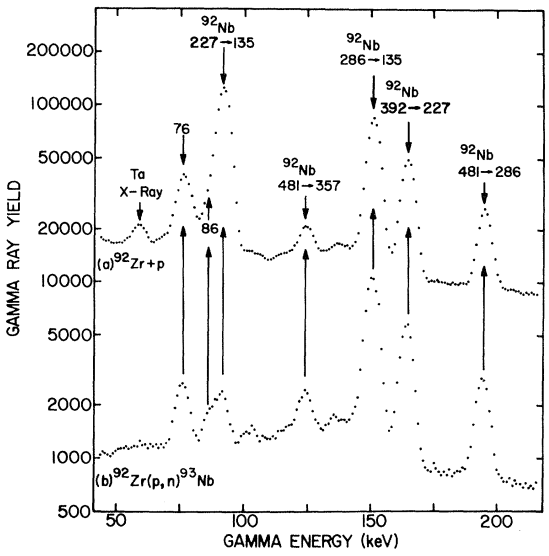

FIG. 5. (a) γ-ray singles spectrum up to 220 keV obtained for $E_p = 6.3$ MeV and $\theta_\gamma = 90°$. (b) γ rays observed in coincidence with neutrons for a resolving time of ~200 nsec.

20° to the beam direction.

For the delayed-coincidence timing measurement, the detector discussed above was used for the neutrons which populate the state, and the γ rays which mark the decay were detected in a 1.5 ×1.5-in. NaI crystal mounted on a RCA 8575 phototube. Fast timing signals from the neutron detector were obtained from the anode. A short delay line at the anode allowed for fast crossover timing which has the advantage of good time resolution for a wide dynamic range in pulse height. For the γ detector the timing signals were obtained from the leading edge of the anode pulses. These timing signals start and stop the TAC 2 as indicated in Fig. 3. Time calibration was made with air-dielectric trombone delay lines.

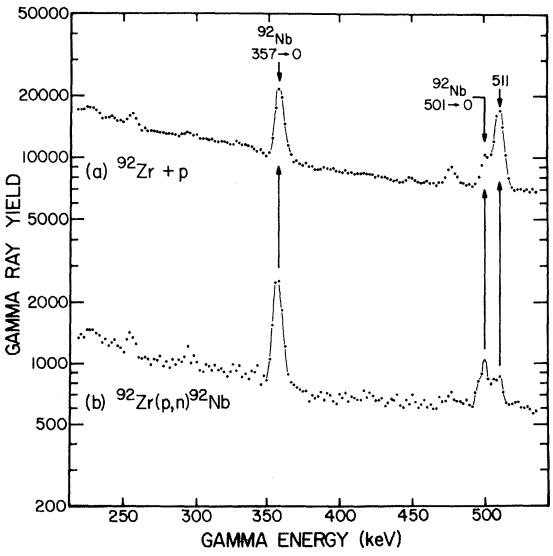

FIG. 6. (a) γ-ray singles spectrum from 220 to 540 keV obtained for $E_p = 6.3$ MeV and $\theta_\gamma = 90°$. (b) γ rays observed in coincidence with neutrons for a resolving time of ~200 nsec.

Slow-coincidence requirements were used in conjunction with the fast timing to isolate the excited state of interest and to minimize the time resolution. To achieve these requirements SCA's were set to select appropriate pulse-height regions from linear dynode pulses. For the neutron detector, SCA 1 was adjusted to accept pulses in the neutron energy region 1.5–3.1 MeV; this eliminated low-energy neutrons that populate high excited states and the intense 511-keV annihilation γ rays. As an additional slow-coincidence requirement, SCA 2 of the neutron discriminator was adjusted to accept a narrow window of the neutron peak as shown in Fig. 4.

For the slow-coincidence requirements on the γ detector, SCA 3 and 4 were both fed by its amplifier AMP 2; SCA 3 accepted only the photopeak of the 357-keV γ ray in its pulse-height window and SCA 4 a region about the same width above the 357-keV photopeak. The outputs of SCA 3 and 4 were also used to route the corresponding time-delay spectra into different halves of a multichannel analyzer. As shown in Fig. 2, the only prominent photopeak in the 200–490-keV energy region is the 357-keV γ transition. Thus, the SCA 4 γ window represents the Compton background portion of the SCA 3 window.

The experimental decay curve for the 357-keV (5^+) state in ^{92}Nb is shown by the filled circles and the solid line in Fig. 7. From several least-squares fits to different portions of the logarithmic slope, the extracted mean lifetime of the 357-keV (5^+) state is $\tau = 2.73 \pm 0.09$ nsec. The dashed line in Fig. 7 shows the time-delay spectrum gated by SCA 4 which guarantees that the Compton background of SCA 3 does not contribute to the 2.73-nsec mean lifetime. The dashed spectrum also represents a simultaneous measurement of an upper limit to the prompt resolution function with an average slope equivalent to $\tau = 0.8$ nsec.

The same experimental approach described above was used for a measurement of the time-delay spectrum for the 501-keV (6^+) state in ^{92}Nb. The observed result gives only an upper limit to the mean lifetime of $\tau \leq 0.8$ nsec. It should be noted that the prompt γ-γ time spectrum is shifted relative to that for n-γ events by $\Delta t = L[(1/v_n) - (1/c)]$, where L is the distance between the neutron detector and the target. For this measurement, $\Delta t \approx 2.5$ nsec. Considerable care must be taken when measuring mean lifetimes $\tau < 1$ nsec to

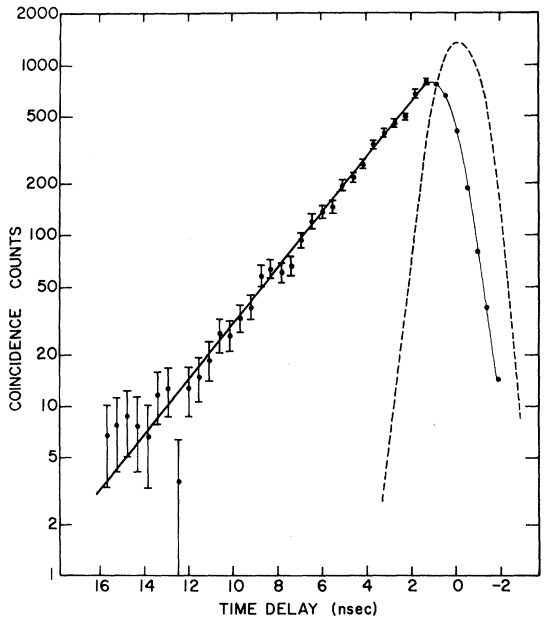

FIG. 7. The experimental decay curve for the 357-keV 5^+ state in ^{92}Nb as shown with filled circles and the solid line. The n-γ time-delay spectrum was obtained relative to neutrons from the ^{92}Zr$(p,n)^{92}$Nb reaction that populate the 357-keV 5^+ state. The left slope of the decay curve corresponds to a mean lifetime $\tau = 2.73 \pm 0.09$ nsec. The dashed line represents the prompt resolution function which has an average slope equivalent to $\tau = 0.8$ nsec.

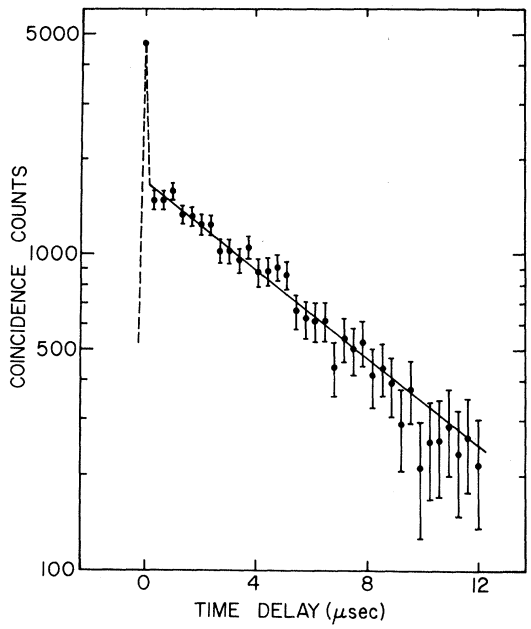

FIG. 8. The experimental decay curve for the 227-keV 2^- state in ^{92}Nb as shown by the filled circles and the solid line. The time-delay spectrum was obtained by a γ-γ measurement between the 165-keV γ ray that cascades from the 392-keV 3^- state and the 92-keV decay γ ray. The right slope of the decay curve corresponds to a mean lifetime $\tau = 6.2 \pm 0.7$ μsec.

avoid γ pulses in the neutron discriminator which might contribute a prompt peak to the n-γ time spectrum.

C. Lifetime Measurement of the 227-keV 2^- State

The singles and the neutron-coincidence γ spectra indicate that the lifetime of the 227-keV 2^- state in ^{92}Nb is in the μsec region. The 2^- state lifetime was measured by a γ-γ delayed-coincidence technique. The time of formation of the 2^- state was determined by the detection of the 165-keV $3^- \rightarrow 2^-$ γ ray in a Ge(Li) detector, while the decay was marked by the detection of the 92-keV $2^- \rightarrow 2^+$ γ ray in a NaI detector. Timing for this measurement was achieved from the bipolar zero crossover of linear photopeak pulses. A start-stop TAC was used to convert the time delays to a pulse-height spectrum. The resulting time spectrum is shown in Fig. 8. A least-squares fit to the observed decay curve resulted in a mean lifetime of $\tau = 6.2 \pm 0.7$ μsec for the 227-keV 2^- state in ^{92}Nb. The prompt resolution function is indicated by the narrow peak at zero time; it was produced by Compton background pulses from higher-energy γ rays that entered the pulse-height windows. In order to check that the observed lifetime is not initiated by start pulses from some of these Compton events, a simultaneous time spectrum was taken with the pulse-height window just below the 165-keV photopeak. This result shows less than a 5% contribution to the long lifetime; this contribution is explained by the 165-keV Compton pulses. In order to insure that the 92-keV γ ray is responsible for the 6.2-μsec mean lifetime, the measurement was repeated using the Ge(Li) detector for the 92-keV γ ray and the NaI detector for the 165-keV γ ray. A similar lifetime result for these conditions indicates unambiguously that the measured lifetime is associated with the 227-keV 2^- state.

III. DISCUSSION

A summary of the experimental lifetime information obtained for the low-lying states of ^{92}Nb is given in Table I. In addition, the excited states at 286,

TABLE I. Mean liftetime results for states in ^{92}Nb.

E (keV)	τ
135	14.7 days [a]
227	6.2 ± 0.7 μsec
357	2.73 ± 0.09 nsec
501	≤ 0.8 nsec

[a] See Refs. 11 and 12.

392, and 481 keV have a mean lifetime of $\tau < 1$ μsec as determined from the resolving time for the neutron-γ coincidence measurement. No prominent photopeak was seen in coincidence for the γ decay of the 135-keV first excited state; this is in agreement with its measured 14.7-days mean lifetime.[11,12]

As pointed out in Sec. I, the level order of the ^{92}Nb sextuplet of positive-parity states with $J = 2$ through 7 is not well-established by the reaction studies. In particular, the 3^+ and 5^+ order is uncertain for the 286- and 357-keV states and also, there is some question about the 4^+ and 6^+ order for the 481- and 501-keV states. The γ-transition probabilities measured in the present experiment determine the level sequence for this expected sextuplet to be $7^+, 2^+, 3^+, 5^+, 4^+, 6^+$, as shown in Fig. 1.

The observed neutron-coincidence γ spectrum for the ^{92}Zr$(p, n\gamma)^{92}$Nb reaction shows strong γ transitions between the states $357 \rightarrow 0$ and $286 \rightarrow 135$, where the energies are given in keV, while the $286 \rightarrow 0$ and $357 \rightarrow 135$ transitions were not observed. Accepting the spin assignments of 2^+ for the 135-keV state and 7^+ for the ground state, these results suggest a 5^+ assignment for the 357-keV state and 3^+ for the 286-keV state. The present mean lifetime results of $\tau(357\ \text{keV}) = 2.73 \pm 0.09$ nsec and $\tau(286\ \text{keV}) < 1$ μsec are consistent with the $5^+ \rightarrow 7^+$ $(357 \rightarrow 0)$ $E2$ transition and a $3^+ \rightarrow 2^+$ $(286 \rightarrow 135)$ $M1$-$E2$ transition, respectively, while the reverse assignments require unreasonable enhancements relative to single-particle estimates of 10^{12} for a $357 \rightarrow 0$ $E4$ transition and of $>10^7$ for a $286 \rightarrow 135$ $M3$ transition. Thus, these results determine the 3^+ and 5^+ members of the ^{92}Nb sextuplet to be at 286 and 357 keV, respectively.

A similar set of arguments applies to the 4^+ and 6^+ order for the 481- and 501-keV states. The neutron-coincidence γ spectrum shows strong $501 \rightarrow 0$, $481 \rightarrow 357$, and $481 \rightarrow 286$ γ transitions, while the $501 \rightarrow 286$ and $481 \rightarrow 0$ transitions were not observed. Using the spin assignments for the lower members of the sextuplet discussed above, these results suggest a 4^+ assignment to the 481-keV state and 6^+ to the 501-keV state. Moreover, the present mean-lifetime information of $\tau(481\ \text{keV}) < 1$ μsec and $\tau(501\ \text{keV}) \leq 0.8$ nsec requires for the reverse assignments completely unreasonable enhancements relative to single-particle estimates of $>10^7$ for a $481 \rightarrow 286$ $M3$ transition and of $>10^8$ for a $501 \rightarrow 0$ $M3$ transition. Hence, the 4^+ member of the sextuplet in ^{92}Nb is the 481-keV state and the 6^+ member is at 501 keV.

The present study of electromagnetic transitions in ^{92}Nb, thus, selects the level order of $7^+, 2^+, 3^+, 5^+, 4^+, 6^+$ for the positive-parity sextuplet. This order is consistent with the residual potential used by Pandya.[10] Also, theoretical predictions[6-8] for low-lying levels in Nb, Mo, and Tc have been carried out with a $1g_{9/2}$-$2d_{5/2}$ interaction which is determined in part by this ^{92}Nb level order.

The $E1$ transitions between the positive-parity sextuplet and the negative-parity doublet in ^{92}Nb are strongly hindered. In fact, none of the $E1$ branches $4^+ \rightarrow 3^-$, $3^- \rightarrow 3^+$, $3^- \rightarrow 2^+$, and $3^+ \rightarrow 2^-$ compete significantly with alternative $M1$ or $E2$ branches as observed in the neutron-coincidence γ spectrum. The mean lifetime measured for the 2^- 227-keV state of $\tau = 6.2 \pm 0.7$ μsec implies an $E1$ hindrance of 10^7 relative to single-particle estimates for the $2^- \rightarrow 2^+$ transition; no competing branches exist for the decay of the 2^- state. This large hindrance is understood by the fact that an $E1$ operator does not connect $2p_{1/2}$ and $1g_{9/2}$ configurations. The value of the $E1$ hindrance implies admixtures with amplitudes $<10^{-3}$; the most likely admixtures are $2d_{3/2}$ or $3s_{1/2}$ proton configurations in the positive-parity states. This result indicates very pure $2p_{1/2}$ and $1g_{9/2}$ proton configurations for the low-lying states in ^{92}Nb.

The mean-lifetime result of $\tau = 2.73 \pm 0.09$ nsec for the 357-keV 5^+ state implies an experimental reduced transition probability $B(E2) = 50.9\ e^2\ \text{F}^4$ for the transition to the 7^+ ground state. The theoretical reduced transition probability for this $E2$ transition has been calculated with the wave functions suggested for the positive-parity sextuplet. Configurations of seniority two $[\nu(1d_{5/2})][\pi(1g_{9/2})]J^+$ were used and the radial part of the matrix element $\langle r^2 \rangle$ for both $\nu(2d_{5/2})$ and $\pi(1g_{9/2})$ were determined with harmonic-oscillator wave functions. The oscillator parameter was chosen by comparing the R_{rms} of ^{90}Zr obtained from electron scattering data[14] with that calculated for particles filling the appropriate harmonic-oscillator shells. The resulting theoretical reduced transition probability is $B(E2) = 7.4(e_\nu + 0.35e_\pi)^2\ \text{F}^4$, where e_ν and e_π are effective charges for a $2d_{5/2}$ neutron and $1g_{9/2}$ proton, respectively. A comparison of this theoretical $B(E2)$ with the experimental value implies that $(e_\nu + 0.35e_\pi) = 2.62e$. Using the $1g_{9/2}$ effective proton charge $e_\pi = (2.1 \pm 0.1)e$, measured[15] in ^{92}Mo,

TABLE II. Experimental $E2$ effective charges in the mass-90 region.

Nucleus	$e_\nu(2d_{5/2})$	$e_\pi(1g_{9/2})$
^{92}Zr	2.1 ± 0.2 [a]	
^{94}Zr	1.9 ± 0.2 [a]	
^{92}Mo		2.1 ± 0.2 [b]
^{92}Nb	1.9 [c]	2.1 [c]

[a] See Ref. 16.
[b] See Ref. 15.
[c] Consistent with $(e_\nu + 0.35\ e_\pi) = 2.62\ e$ obtained from present experiment.

the above relation yields a $2d_{5/2}$ effective neutron charge of $e_\nu = (1.9 \pm 0.2)e$. This value is in agreement with previous measurements[16] for the $2d_{5/2}$ effective neutron charge, $e_\nu = 2.1 \pm 0.2e$ in ^{92}Zr and $1.9 \pm 0.2\ e$ in ^{94}Zr. The $E2$ effective charge information for this mass region is listed in Table II. Thus, this 357-keV $5^+ \rightarrow 7^+$ $E2$ transition in ^{92}Nb is consistent with $[\nu(2d_{5/2})][\pi(1g_{9/2})]J^+$ wave functions.

In summary, the present experiment selects the 3^+-5^+ and 4^+-6^+ order of the positive-parity sextuplet in ^{92}Nb as shown in Fig. 1. The measured $E1$ and $E2$ strengths in ^{92}Nb are consistent with the theoretically suggested $\pi(1g_{9/2})$, $\pi(2p_{1/2})$, and $\nu(2d_{5/2})$ shell-model configurations.

ACKNOWLEDGMENT

The authors wish to acknowledge helpful discussions with Dr. J. Blomquist.

---

†Work supported in part by the National Science Foundation.

[1]R. K. Sheline, C. Watson, and W. E. Hamburger, Phys. Letters 8, 121 (1964).

[2]R. F. Sweet, K. H. Bhatt, and J. B. Ball, Phys. Letters 8, 131 (1964).

[3]M. R. Cates, J. B. Ball, and E. Newman, Phys. Rev. 187, 1682 (1969).

[4]A. de-Shalit, Phys. Rev. 91, 1479 (1953).

[5]Y. E. Kim, Phys. Rev. 131, 1712 (1963).

[6]N. Auerbach and I. Talmi, Nucl. Phys. 64, 458 (1965).

[7]K. H. Bhatt and J. B. Ball, Nucl. Phys. 63, 286 (1965).

[8]J. Vervier, Nucl. Phys. 75, 17 (1966).

[9]R. K. Sheline, R. T. Jernigan, J. B. Ball, K. H. Bhatt, Y. E. Kim, and J. Vervier, Nucl. Phys. 61, 342 (1965).

[10]S. P. Pandya, Phys. Letters 10, 178 (1964).

[11]C. M. Lederer, J. M. Hollander, and I. Perlman, *Table of Isotopes* (John Wiley & Sons, Inc., New York, 1967), 6th ed.

[12]M. E. Bunker, B. J. Dropesky, J. D. Knight, and J. W. Starner, Phys. Rev. 127, 844 (1962).

[13]M. L. Roush, M. A. Wilson, and W. F. Hornyak, Nucl. Instr. Methods 31, 112 (1964).

[14]J. Belicard, P. Leconte, T. H. Curtis, R. A. Eisenstein, D. Madsen, and C. Bockelman, Nucl. Phys. A143, 213 (1970).

[15]S. Cochavi, J. M. McDonald, and D. B. Fossan, to be published.

[16]S. Cochavi, N. Cue, and D. B. Fossan, Phys. Rev. C 1, 1821 (1970).